



# Medium dynamics in heavy-ion collisions at the NICA energies within the PHSD model

*Phys.Rev.C* 107 (2023) 3 & *Particles* 6 (2023) 1 &  
*Particles* 7 (2024) 4 & *Phys.Rev.C* 111 (2025) 3 &  
[arXiv:2502.10146](https://arxiv.org/abs/2502.10146)

N. Tsegelnik<sup>1,2,\*,†</sup>, E. Kolomeitsev<sup>1,3</sup>,  
V. Voronyuk<sup>4</sup>,

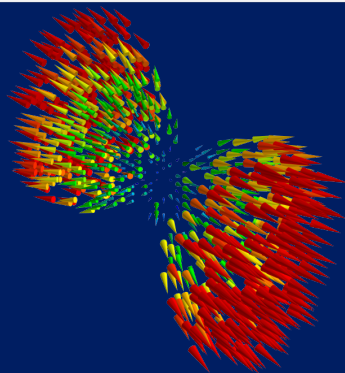
G. Prokhorov<sup>1,2</sup>, D. Shohonov<sup>1</sup>,  
O. Teryaev<sup>1,2</sup>, V. Zakharov<sup>2,1</sup>

\*[tsegelnik@jinr.ru](mailto:tsegelnik@jinr.ru)

5 July 2025



umb MATEJ BEL  
UNIVERSITY



<sup>1</sup>Laboratory of Theoretical Physics, JINR, Dubna, Russia

<sup>2</sup>NRC Kurchatov Institute, Moscow, Russia

<sup>3</sup>Matej Bel University, Banská Bystrica, Slovakia

<sup>4</sup>Laboratory of High Energy Physics, JINR, Dubna, Russia

<sup>†</sup> The research supported by the grants for young scientists and specialists of JINR № 25-301-06

# The introduction and motivation

*The Most Intriguing Fluid in Nature*



# The strongly interacting nearly ideal fluid



ELSEVIER

Available online at [www.sciencedirect.com](http://www.sciencedirect.com)

SCIENCE @ DIRECT®



Nuclear Physics A 757 (2005) 1–27

## Quark–gluon plasma and color glass condensate at RHIC? The perspective from the BRAHMS experiment

### Abstract

We review the main results obtained by the BRAHMS Collaboration on the properties of hot and dense hadronic and partonic matter produced in ultrarelativistic heavy ion collisions at RHIC. A particular focus of this paper is to discuss to what extent the results collected so far by BRAHMS, and by the other three experiments at RHIC, can be taken as evidence for the formation of a state of deconfined partonic matter, the so-called quark–gluon plasma (QGP). We also discuss evidence for a possible precursor state to the QGP, i.e., the proposed color glass condensate.



ELSEVIER

Available online at [www.sciencedirect.com](http://www.sciencedirect.com)

SCIENCE @ DIRECT®



Nuclear Physics A 757 (2005) 102–183

## Experimental and theoretical challenges in the search for the quark–gluon plasma: The STAR Collaboration's critical assessment of the evidence from RHIC collisions

STAR Collaboration

### Abstract

We review the most important experimental results from the first three years of nucleus–nucleus collision studies at RHIC, with emphasis on results from the STAR experiment, and we assess their interpretation and comparison to theory. The theory–experiment comparison suggests that central Au + Au collisions at RHIC produce dense, rapidly thermalizing matter characterized by: (1) initial energy densities above the critical values predicted by lattice QCD for establishment of a quark–gluon plasma (QGP); (2) nearly ideal fluid flow, marked by constituent interactions of very short mean free path, established most probably at a stage preceding hadron formation; and (3) opacity to jets. Many of the observations are consistent with models incorporating QGP formation in the early collision stages, and have not found ready explanation in a hadronic framework. However, the



ELSEVIER

Available online at [www.sciencedirect.com](http://www.sciencedirect.com)

SCIENCE @ DIRECT®



Nuclear Physics A 757 (2005) 28–101

## The PHOBOS perspective on discoveries at RHIC

PHOBOS Collaboration

### Abstract

This paper describes the conclusions that can be drawn from the data taken thus far with the PHOBOS detector at RHIC. In the most central Au + Au collisions at the highest beam energy, evidence is found for the formation of a very high energy density system whose description in terms of simple hadronic degrees of freedom is inappropriate. Furthermore, the constituents of this novel system are found to undergo a significant level of interaction. The properties of particle production at RHIC energies are shown to follow a number of simple scaling behaviors, some of which continue trends found at lower energies or in simpler systems. As a function of centrality, the total number



ELSEVIER

Available online at [www.sciencedirect.com](http://www.sciencedirect.com)

SCIENCE @ DIRECT®



Nuclear Physics A 757 (2005) 184–283

## Formation of dense partonic matter in relativistic nucleus–nucleus collisions at RHIC: Experimental evaluation by the PHENIX Collaboration

PHENIX Collaboration

### Abstract

Extensive experimental data from high-energy nucleus–nucleus collisions were recorded using the PHENIX detector at the Relativistic Heavy Ion Collider (RHIC). The comprehensive set of measurements from the first three years of RHIC operation includes charged particle multiplicities, transverse energy, yield ratios and spectra of identified hadrons in a wide range of transverse momenta ( $p_T$ ), elliptic flow, two-particle correlations, nonstatistical fluctuations, and suppression of particle production at high  $p_T$ . The results are examined with an emphasis on implications for the formation of a new state of dense matter. We find that the state of matter created at RHIC cannot be described in terms of ordinary color neutral hadrons.



## NEWS & VIEWS

For News & Views online, go to  
[nature.com/newsandviews](https://www.nature.com/newsandviews)

*Nature* **548**, 34–35 (2017)

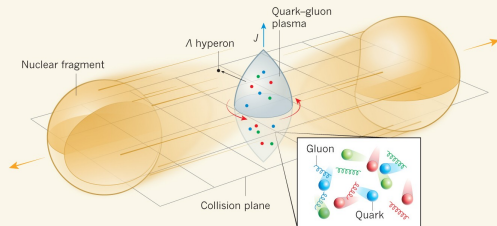
### NUCLEAR PHYSICS

## The fastest-rotating fluid

A state of matter called a quark–gluon plasma is produced in energetic collisions of heavy ions. The rotation of this plasma has been measured for the first time, providing insights into the physics of the strong nuclear force. [SEE LETTER P.62](#)

HANNAH PETERSEN

- The collective dynamics of heavy-ion collisions can produce emergent phenomena, like *spin polarization*.
- The observed global polarization of  $\Lambda$  and  $\bar{\Lambda}$  in heavy-ion collisions suggests that a quark–gluon plasma may be *the fastest-rotating fluid in nature*.







## Our research in words

---

acceleration  
fluid  
medium  
mesons  
freeze-out conditions  
hyperons  
QGP  
phase transitions  
the Unruh temperature  
fireball  
heavy-ion collisions  
vorticity  
spin polarization  
strangeness production

# The setup

*The PHSD transport model, centrality definition and temperatures from the blast-wave model*

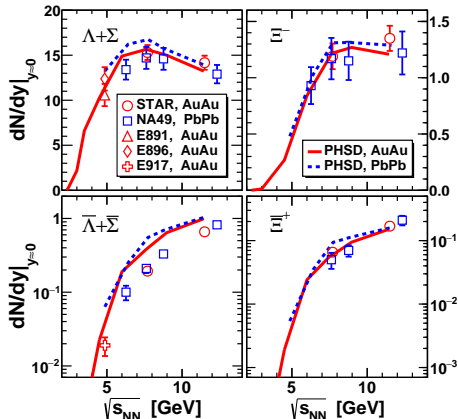


# The PHSD transport model

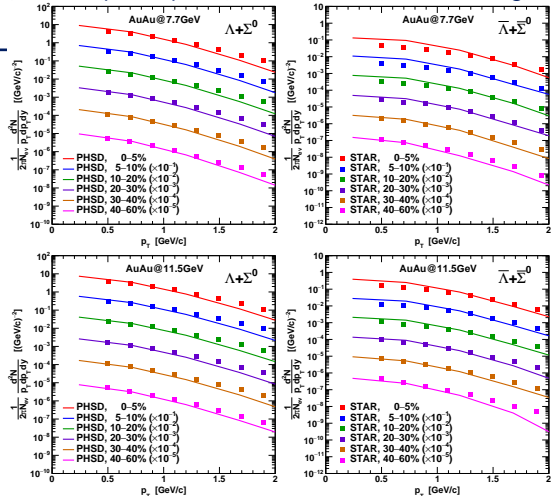


The **PHSD transport model**<sup>†</sup> as a heavy-ion collisions framework: based on **the Kadanoff-Baym equations** (on-shell and off-shell dynamics, first gradient expansion, test particles ansatz), **DQPM** (parton phase), **FRITIOF Lund** (hard scattering), **Chiral Symmetry Restoration** (strangeness production), ...

<sup>†</sup>W. Cassing, E.L. Bratkovskaya, Phys. Rev. C 78 (2008); Nucl. Phys. A 831 (2009); ...



V. Voronyuk, N.S. Tsegelnik, E.E. Kolomeitsev, Phys.Rev.C 111 (2025) 3



N. Tsegelnik, E. Kolomeitsev, V. Voronyuk, Particles 6 (2023) 1

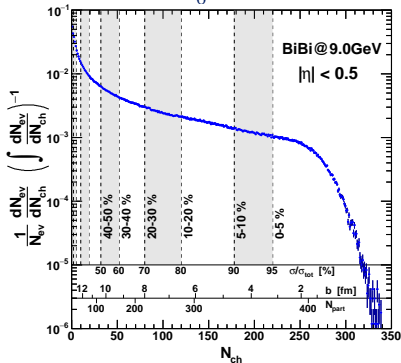


# The centrality definition and hyperons hierarchy

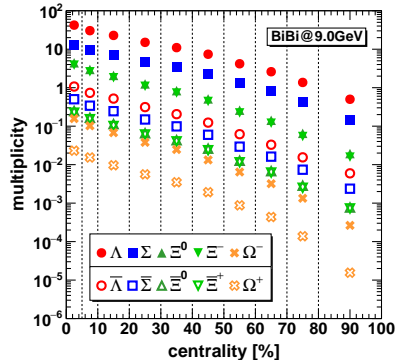


- We define centrality classes via integrals of the events distribution:

$$C = \frac{1}{N_{ev}} \int_0^{N_{ch}} \frac{dN_{ev}}{dN_{ch}} dN_{ch}.$$



- For the most central collisions (0 – 5% centrality):



$$M_{\Lambda} : M_{\Xi} : M_{\Omega} = 1 : 10^{-1} : 4 \times 10^{-3}$$

$$M_{\bar{\Lambda}} : M_{\bar{\Xi}} : M_{\bar{\Omega}} = 1 : 2 \times 10^{-1} : 2 \times 10^{-2}$$

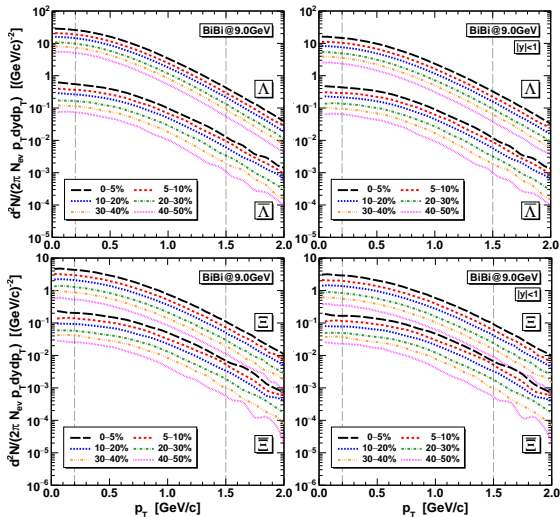
- PbPb@8.77GeV, 0 – 7% centrality (NA49):

$$M_{\Lambda} : M_{\Xi} : M_{\Omega} = 1 : (7 \pm 1.0) \times 10^{-2} : (3 \pm 2) \times 10^{-3}$$

$$M_{\bar{\Lambda}} : M_{\bar{\Xi}} = 1 : (2 \pm 0.5) \times 10^{-1}$$



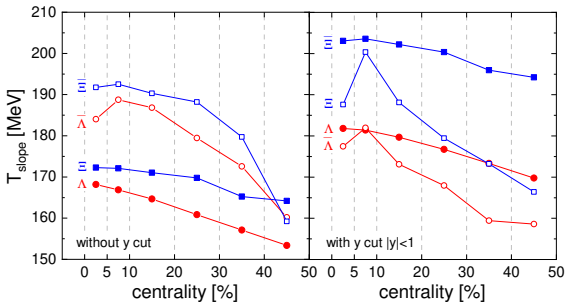
# Temperatures from the blast-wave model



N. Tsekelink, V. Voronyuk, E. Kolomeitsev, *Particles* 7 (2024) 4

- To find the slopes we fit the distributions with the **blast-wave formula** ( $0.5 \leq p_T \leq 1.5$  GeV):

$$\frac{dN}{2\pi p_T dp_T} = A m_T K_1\left(\frac{m_T}{T_{\text{slope}}}\right), \quad m_T = \sqrt{m_H^2 + p_T^2}.$$



- For hyperons  $T_{\text{slope}}$  shows weak dependence on the centrality decreasing by  $\sim 5 - 15$  MeV.
- For anti-hyperons a decrease is stronger (by  $\sim 30$  MeV).
- The cut  $|y| < 1$  leads to an increase of  $T_{\text{slope}}$  by 13 – 17 MeV for  $\Lambda$ s and by 30 MeV for  $\Xi$ s.

# The medium dynamics

*The particles-to-medium transition, velocity, vorticity, acceleration and the Unruh temperature*



# The particles-to-medium transition



particles-to-medium transition  $\longleftrightarrow$  fluidization  $\longleftrightarrow$  continuization  $\longleftrightarrow$  collectivization

- Transition from kinetic to hydrodynamic variables via the *effective fluidization* procedure:

$$T^{\mu\nu}(\mathbf{x}, t) = \frac{1}{\mathcal{N}} \sum_{a, i_a} \frac{p_{i_a}^{\mu}(t) p_{i_a}^{\nu}(t)}{p_{i_a}^0(t)} \Phi(\mathbf{x}, \mathbf{x}_{i_a}(t)),$$

$$\mathcal{N} = \int \Phi(\mathbf{x}, \mathbf{x}_i(t)) d^3x,$$

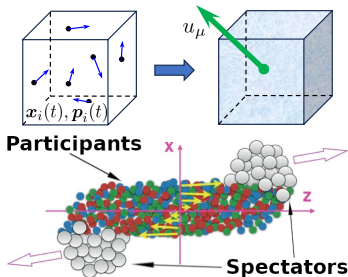
$$J_B^{\mu}(\mathbf{x}, t) = \frac{1}{\mathcal{N}} \sum_{a, i_a} B_{i_a} \frac{p_{i_a}^{\mu}(t)}{p_{i_a}^0(t)} \Phi(\mathbf{x}, \mathbf{x}_{i_a}(t)),$$

$\Phi(\mathbf{x}, \mathbf{x}_i(t))$  – smearing function,

$$u_{\mu} T^{\mu\nu} = \varepsilon u^{\nu}, \quad n_B = u_{\mu} J_B^{\mu}, \quad \longrightarrow \quad \text{EoS}^a \quad \longrightarrow$$

Temperature( $\varepsilon, n_B$ )

- The fluidization criterion:  
only cells with  $\varepsilon \geq \varepsilon_f \approx 0.05 \text{ GeV/fm}^3$ !
- Spectators separation:  
spectators do not interact and do not form fluid!
- N.S. Tsengelk, E.E. Kolomeitsev, V. Voronyuk, *Phys.Rev.C* **107** (2023) 3



<sup>a</sup> Hadron resonance gas: L.M. Satarov, M.N. Dmitriev, and I.N. Mishustin, *Phys. Atom. Nucl.* **72** (2009)

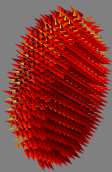


# The velocity and vorticity fields

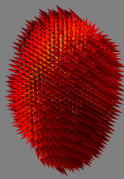


AuAu@7.7GeV,  $b=7.5\text{fm}$

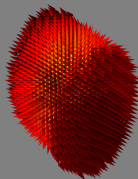
AuAu@7.7GeV,  $b=7.5\text{fm}$ ,  $t=5.0\text{fm}/c$



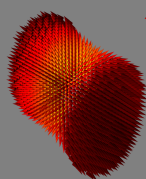
AuAu@7.7GeV,  $b=7.5\text{fm}$ ,  $t=7.0\text{fm}/c$



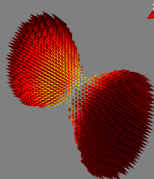
AuAu@7.7GeV,  $b=7.5\text{fm}$ ,  $t=9.0\text{fm}/c$



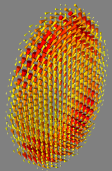
AuAu@7.7GeV,  $b=7.5\text{fm}$ ,  $t=11.0\text{fm}/c$



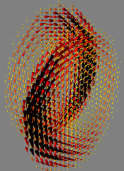
AuAu@7.7GeV,  $b=7.5\text{fm}$ ,  $t=13.0\text{fm}/c$



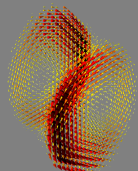
AuAu@7.7GeV,  $b=7.5\text{fm}$ ,  $t=5.0\text{fm}/c$



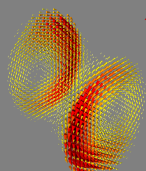
AuAu@7.7GeV,  $b=7.5\text{fm}$ ,  $t=7.0\text{fm}/c$



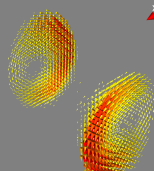
AuAu@7.7GeV,  $b=7.5\text{fm}$ ,  $t=9.0\text{fm}/c$



AuAu@7.7GeV,  $b=7.5\text{fm}$ ,  $t=11.0\text{fm}/c$



AuAu@7.7GeV,  $b=7.5\text{fm}$ ,  $t=13.0\text{fm}/c$



N. Tegelink, E. Kolomeitsev, V. Voronyuk, *Particles* 6 (2023) 1

vorticity:  $\omega = \nabla \times \mathbf{v}$

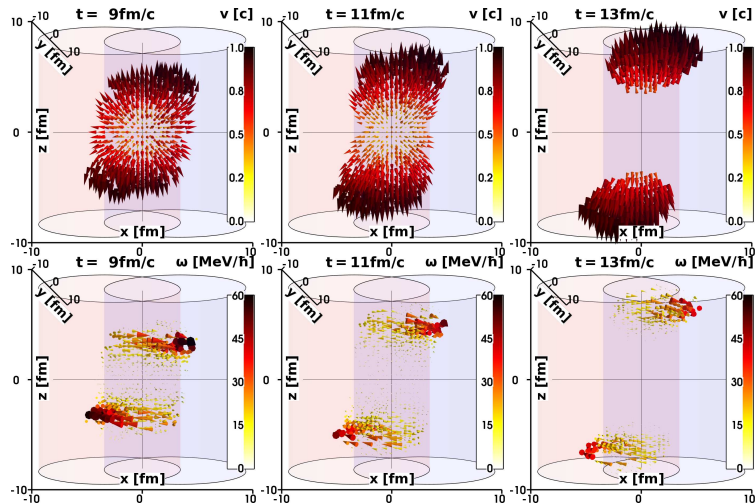




# The velocity and vorticity fields



BiBi@9.06eV,  $b=8.5\text{fm}$

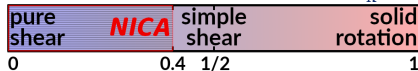


- $\approx$  The Hubble (2+1)D expansion
- Two deformed (due to impact parameter) elliptical **vortex rings** move and rotate in opposite directions along the collision axis.
- The vorticity magnitude reaches  $\sim 80\text{ MeV}/\hbar$  in dynamics!
- The kinematic vorticity number:

$$V_k = \frac{2}{\pi} \arctan \frac{|\omega|}{\sqrt{2}\xi}$$

$$\xi^2 = (\partial_i v_j + \partial_j v_i)(\partial^i v^j + \partial^j v^i)/4$$

Flow characterization via  $V_k$





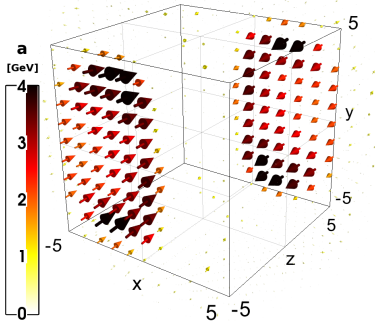
# The acceleration

$$a_\mu = u^\nu \partial_\nu u_\mu = (a^0, \mathbf{a})$$



full system

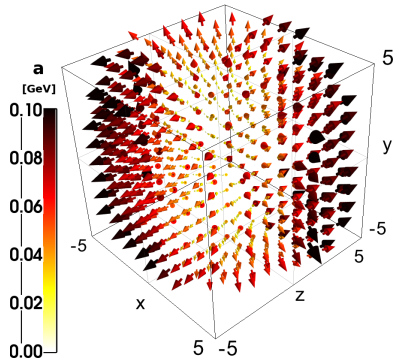
Au+Au at  $\sqrt{s_{NN}} = 7.7 \text{ GeV}$ ,  $b = 7.5 \text{ fm}$ ,  $t - t_{\text{coll}} = 5.0 \text{ fm/c}$



- The maximum magnitude ( $a \sim 2 - 5 \text{ GeV}$ ) is located at the system edge at  $z = z_{\text{max}}$ .
- These zones are characterized by an *extremely high deceleration due to the relativistic stopping*.
- G.Yu. Prokhorov, D.A. Shohonov, O.V. Teryaev, N.S. Tsegelnik, V.I. Zakharov, arXiv:2502.10146; will be in the published version

fireball  $\epsilon_f > 0.05 \text{ GeV/fm}^3$

Au+Au at  $\sqrt{s_{NN}} = 7.7 \text{ GeV}$ ,  $b = 7.5 \text{ fm}$ ,  $t - t_{\text{coll}} = 5.0 \text{ fm/c}$



- The maximum magnitude ( $a \sim 0.1 \text{ GeV}$ ) is located near the edge at  $z = z_{\text{max}} - \delta z$ .
- These zones are characterized by a *smaller acceleration, co-directed within expansion*.
- unpublished; in preparation...



# The Unruh temperature

$$T_U = \sqrt{-a^\mu a_\mu} / 2\pi$$

For QGP and fireball, except the first moments, where  $\langle T_U \rangle_{\text{vol}}$  may be close to  $\langle T \rangle_{\text{vol}}$ :

$$\langle T_U \rangle_{\text{vol}} < \langle T \rangle_{\text{vol}}.$$

For hadrons, except  $t - t_{\text{coll}} = 5 - 10 \text{ fm}/c$  at  $\sqrt{s_{NN}} < 11.5 \text{ GeV}$ , where  $\langle T_U \rangle_{\text{vol}} \approx \langle T \rangle_{\text{vol}}$ :

$$\langle T_U \rangle_{\text{vol}} > \langle T \rangle_{\text{vol}}.$$

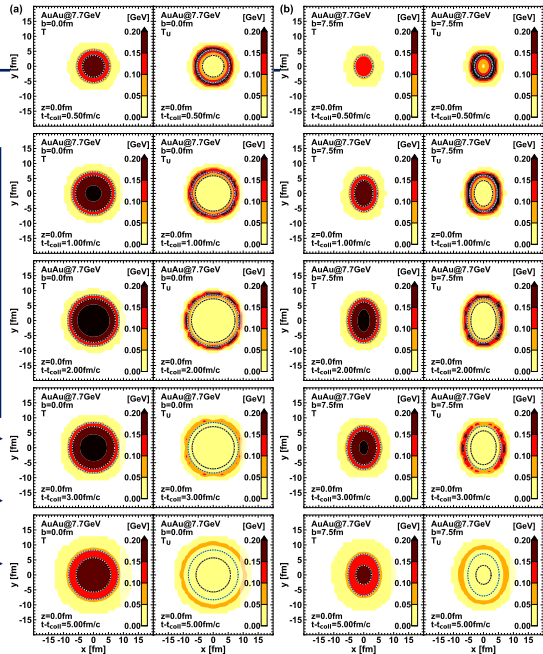
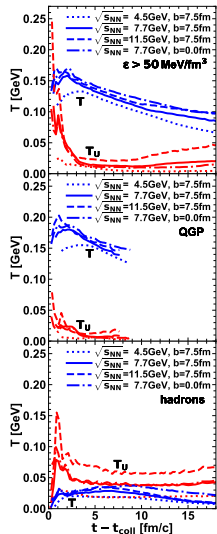
Qualitatively, the picture is independent of the parameters of the colliding system.

Inner black-and-white contour for the QGP phase ( $\epsilon_{\text{QGP}} > 0.5 \text{ GeV}/\text{fm}^3$ ).

Outer blue-and-green contour for the fireball ( $\epsilon_f > 50 \text{ MeV}/\text{fm}^3$ ).

$T_U \geq T$  only for the boundary layer around the fireball.

• G.Yu. Prokhorov, D.A. Shohonov, O.V. Teryaev, N.S. Tsegelnik, V.I. Zakharov, arXiv:2502.10146



# The global polarization

*The vorticity-induced spin polarization and the experimental imprint for the vorticity*



## ■ The thermodynamic approach

*F. Becattini, V. Chandra, L. Del Zanna, E. Grossi, Annals Phys. 338 (2013)*

*Relativistic thermal vorticity:*

$$\varpi_{\mu\nu} = \frac{1}{2}(\partial_\nu\beta_\mu - \partial_\mu\beta_\nu), \quad \beta_\nu = \frac{u_\nu}{T}$$

*Spin vector:*

$$S^\mu(x, p) = -\frac{s(s+1)}{6m}(1 \pm n(x, p))\varepsilon^{\mu\nu\lambda\delta}\varpi_{\nu\lambda}p_\delta$$

$n(x, p)$ — distribution function,  $s$ — spin,  
 $m$ — mass,  $p_\delta$ — 4 momentum of particle

*Spin vector in the particle rest frame:*

$$\mathbf{S}^* = \mathbf{S} - \frac{(\mathbf{S} \cdot \mathbf{p})\mathbf{p}}{E(E + m)}$$

*Polarization:*  $\mathbf{P} = \mathbf{S}^*/s$

## ■ Our algorithm:

1. At each time step we fluidize the system (*excluding spectators*) and calculate the vorticity tensor.

*Medium:*  $\varepsilon > \varepsilon_f \approx 0.05 \text{ GeV/fm}^3$  and  $\varpi_{\mu\nu} \neq 0$ .

*Out of medium:*  $\varepsilon \leq \varepsilon_f \approx 0.05 \text{ GeV/fm}^3$  and  $\varpi_{\mu\nu} = 0$ .

2. After any collision (elastic or inelastic) a particle is polarized by  $\varpi_{\mu\nu}$ .

*In out of medium the polarization is zero due to  $\varpi_{\mu\nu} = 0$ .*

3. **Feed-down:**

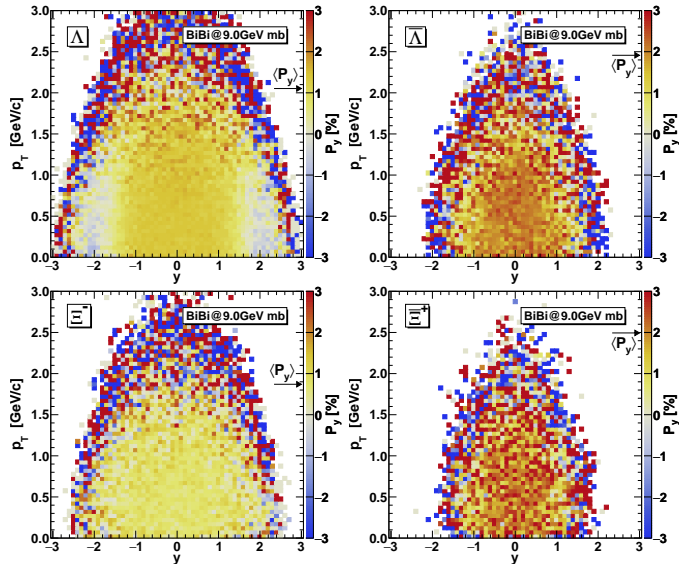
*Strong decays:*  $\Sigma^* \rightarrow \Lambda + \pi, \quad \Xi^* \rightarrow \Xi + \pi$   
*are already taken into account* in the PHSD dynamic  
( $C_{\Lambda\Sigma^*} = C_{\Xi\Xi^*} = 1/3$ ).

*EW decays:*  $\Xi \rightarrow \Lambda + \pi, \quad \Sigma \rightarrow \Lambda + \gamma$   
we consider *by hand* with  $C_{\Lambda\Sigma^0} = -1/3, C_{\Lambda\Xi^0} = 0.914,$   
and  $C_{\Lambda\Xi^0} = 0.943$ .

$\Lambda, \Sigma^0, \Xi^0, \Xi^-, \Omega^-$  (with antiparticles) are stable in PHSD.



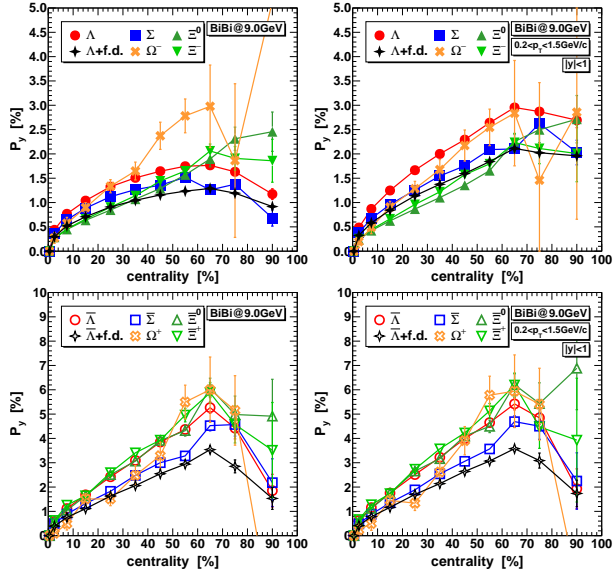
# Polarization map



- Plateau in midrapidity and small momentum  $\longleftrightarrow$  *homogeneous medium*.
- Large fluctuations at high rapidities and momenta  $\longrightarrow$  *zero averaged polarization* for these zones.
- *The averaged polarization of antiparticles is  $\sim 2$  times larger!*
- N. Tsegelink, V. Voronyuk, E. Kolomeitsev, *Particles* 7 (2024) 4



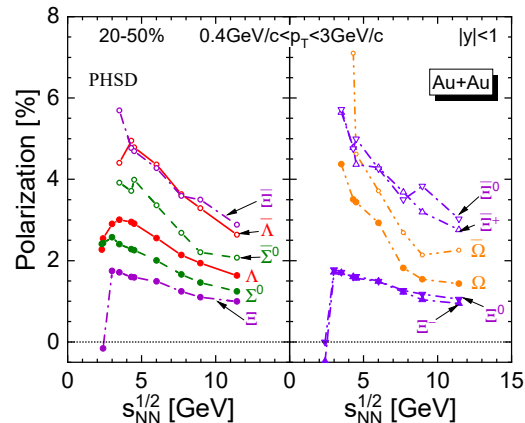
# Polarization vs. centrality



- There is a *different polarization* for particles and antiparticles *for all the hyperon species*.
- The polarization *increases* until the 60 – 70% centrality class and then *decreases* for all the hyperon species.
- The  $p_T$  and  $y$  cuts increase polarization for hyperons, but not for anti-hyperons!*
- The feed-down contribution *decreases* the total polarization of  $\Lambda$  and  $\bar{\Lambda}$  by  $\lesssim 30\%$ . The contamination mostly comes from  $\Sigma^0$  and  $\bar{\Sigma}^0$  due to  $C_{\Lambda\Sigma^0} = -1/3!$
- N. Tsegelnk, V. Voronyuk, E. Kolomeitsev, Particles 7 (2024) 4*



# Polarization vs. collision energy



- The following polarization hierarchy holds for the energy range  $\sqrt{s_{NN}} = 3.5 - 11.5$  GeV:

$$P_{\Xi^-} \approx P_{\bar{\Lambda}} > P_{\Sigma^0} > P_{\Lambda} > P_{\Sigma^0} > P_{\Xi}.$$

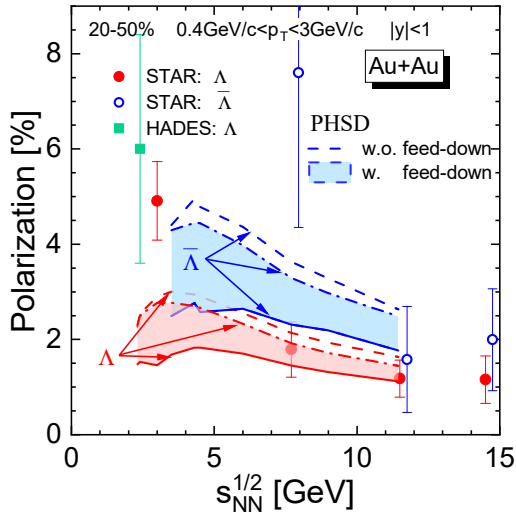
- V. Voronyuk, N.S. Tegelink, E.E. Kolomeitsev, *Phys.Rev.C* **111** (2025) 3

- There is a **different polarization** for particles and antiparticles for all the hyperon species.
- The polarization of all the hyperon kinds **decreases with an energy increase** for  $\sqrt{s_{NN}} > 3 - 4$  GeV.
- The **strongest decrease** and **smallest difference** are for  $\Omega$  and  $\bar{\Omega}$ .
- The **biggest difference** is for  $\Xi$  and  $\bar{\Xi}$ .
- The maximum of  $\Lambda$  and  $\bar{\Lambda}$  polarization occurs at  $\sqrt{s_{NN}} \approx 4$  GeV.





# The feed-down and $\Lambda - \Sigma$ ambiguity



- The polarization of  $\Lambda$  hyperons *agrees* with experimental data, *except low energies*. The polarization of  $\bar{\Lambda}$  is *larger in 1.5 – 2 times* than  $\Lambda$ .
- The filled area reflects uncertainty between ratio of  $\Lambda$ s and  $\Sigma$ s. The limiting case when all  $\Sigma$ s are actually  $\Lambda$ s is depicted via dash-dotted line.
- *It looks more attractive to consider the global polarization of  $\Xi$  hyperons*, which experimentally could be *clearly identified* and would carry *direct information about the spin polarization of the fireball*.
- Moreover, a part of  $\Xi$  comes from  $\Xi^*$  decays and *carries by factor 5/3 stronger polarization than primary  $\Xi$ s*.
- V. Voronyuk, N.S. Tsegelnik, E.E. Kolomeitsev, *Phys.Rev.C* **111** (2025) 3



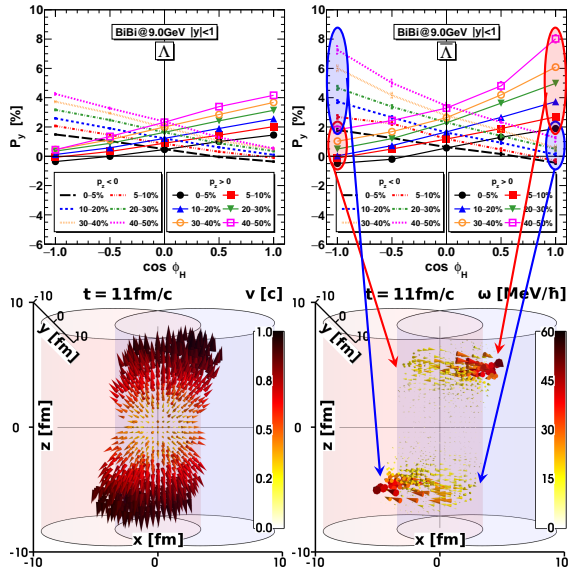
# The vorticity imprint



$$\phi_H = \text{atan}(p_y/p_x)$$

$$\cos \phi_H = p_x/p_T$$

- The highest polarization corresponds to the particles *moving in the same direction as the projectile* (target), which *are mostly born from the matter of the projectile* (target)!
- We can increase the polarization signal by selecting particles by angle and momentum.
- *The imprint of the vorticity mechanism is the angular dependence of the polarization!*
- N. Tsegelink, V. Voronyuk, E. Kolomeitsev, *Particles* **7** (2024) 4

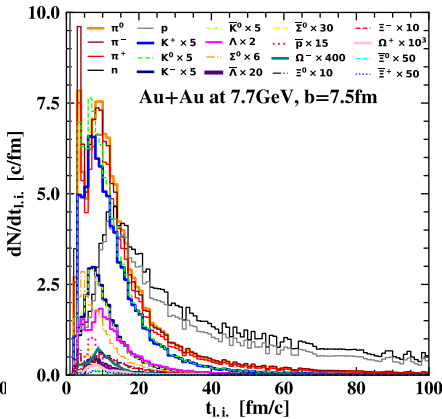
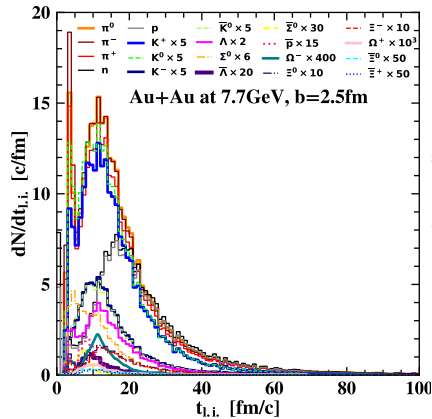


# The freeze-out

*The medium properties of the particles at the last interaction point*



# When particles are interacted last time?



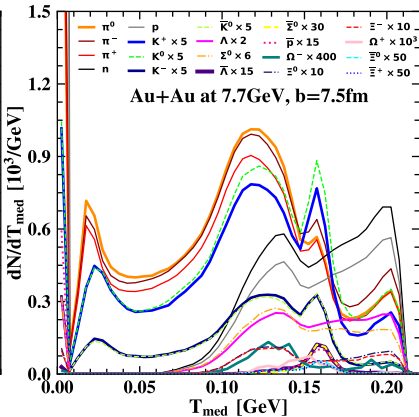
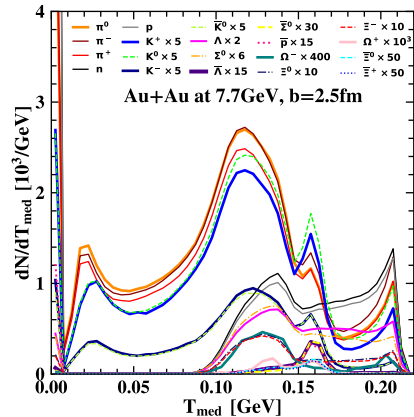
Two peaks:

1. *hard scatterings* in very *dense and hot* cells, *small fireball volume* mostly in the *transverse direction* and small extension in the collision axis (*z-direction*);
2. *main dynamics* of the fireball, maximum  $\approx$  at the moment of the *fireball splitting* into two parts.

- *Hyperons,  $\pi^\pm, \pi^0, K^+, K^0$*  mostly come from these *two peaks*.
- *Anti-hyperons,  $K^-, \bar{K}^0$*  fly away mostly at the moment *between* the peaks.
- *unpublished; in preparation*
- Only for (anti-)hyperons see: *N. Tsegelnk, E. Kolomeitsev, V. Voronyuk, Particles 6 (2023) 1*



# The medium temperature at the particles freeze-out



- Pions, kaons feel the entire medium.
- Hyperons, participant nucleons come from hot medium with broad temperatures distribution  $T_{\text{med}} \approx 0.1 - 0.2$  GeV.
- Antihyperons,  $\bar{p}$  fly away from hot medium with narrow temperatures range around  $T_{\text{med}} \approx 0.16$  GeV.
- unpublished; in preparation

Four peaks:

1.  $T_{\text{med}} \approx 0.02$  GeV: least dense zones;
2.  $T_{\text{med}} \approx 0.05 - 0.15$  GeV: main fireball dynamics  $t \approx 5 - 20$  fm/c;
3.  $T_{\text{med}} \approx 0.16$  GeV: the anti-hyperons and  $\bar{p}$  source,  $t \approx 5 - 10$  fm/c;
4.  $T_{\text{med}} \approx 0.21$  GeV: hard scatterings at  $t \approx 2 - 5$  fm/c.

# Conclusions

*Let's summarize our results*



# Conclusions



- There is good correspondence between the **PHSD** yields and the experimental data.
- The spectra suggest that *anti-hyperons decouple from the fireball earlier than hyperons.*
- We developed a **particles-to-medium transition**  $\longleftrightarrow$  kinetic to (effective) hydrodynamic variables.
- We observed *two deformed elliptic vortex rings*. The deformation depends on the impact parameter.
- We analyzed a measure of the rotationality and concluded that *the flow is mostly irrotational.*
- For the full system the largest acceleration (*deceleration*) is located at *the edges of the system at  $z = z_{\max}$ .*
- For the fireball the largest acceleration (*co-directed within expansion*) is located *near the system edge at  $z = z_{\max} - \delta z$ .*
- We found that  $\langle T_U \rangle_{\text{vol}} \geq \langle T \rangle_{\text{vol}}$  *for the hadrons.*
- We observe that  $\langle T_U \rangle_{\text{vol}} < \langle T \rangle_{\text{vol}}$  *for the QGP and fireball.*
- We found that *polarization for anti-particles is larger than for particles* and *the polarization decrease with an energy increase* for all the hyperon species. *The most contamination in the feed-down account comes from  $\Sigma^0$  and  $\bar{\Sigma}^0$ .*
- We observed that *the polarization increases with centrality* up to 60 – 70% centrality class and then decreases.
- The vorticity mechanism *leads to different polarizations of particles and antiparticles without any additional assumption of different effects on them.* *The polarization trends are consistent with the experimental data.*
- We found that *the angular dependence of the polarization is an imprint of the vorticity mechanism.* *Selecting particles by angles and the sign of  $p_z$ , we can increase the polarization signal.*
- We found that *mesons* feel the *entire medium*, *hyperons*, *participant nucleons* come from the *hot medium* with a *broad* temperatures distribution, *anti-hyperons* fly away from the *hot medium* with *narrow* temperatures range.
- We investigated the polarization sources and confirmed that the anti-hyperons and hyperons have *different thermodynamic conditions at freeze-out*, what *leads to different polarizations.*